IEEE Access
Multidisciplinary ⋮ Rapid Review ⋮ Open Access Journal

Received 2 November 2023, accepted 22 November 2023, date of publication 24 November 2023,
date of current version 30 November 2023.

Digital Object Identifier 10.1109/ACCESS.2023.3336816

RESEARCH ARTICLE

Influence of Load Modeling on the Cost of Ensuring Stability Using TSCOPF

FRANCISCO ARREDONDO[1], MICHAIL RACHMANIDIS[2], PABLO LEDESMA[1], EDGARDO D. CASTRONUOVO[1], (Senior Member, IEEE), AND MOHAMMADAMIN AGHAHASSANI[3]

[1]Departamento de Ingeniería Eléctrica, Universidad Carlos III de Madrid, 28911 Leganés, Spain
[2]DSS Laboratory, EPU-NTUA, National Technical University of Athens, 157 73 Athens, Greece
[3]CITCEA-UPC, Universitat Politècnica de Catalunya, 08028 Barcelona, Spain

Corresponding author: Francisco Arredondo (Francisco.arredondo@uc3m.es)

This work was supported by the Spanish Agencia Estatal de Investigación under Project PID2019-104449RB-I00 and Project AEI/10.13039/501100011033.

ABSTRACT Load modeling significantly impacts the time-domain response of power systems in transient stability studies but this effect is often underestimated in Transient Stability Constrained Optimal Power flow (TSCOPF) studies. The object of this study is twofold: 1) it proposes a robust formulation based on a relevant node representation approach that allows the use of any type of load model in TSCOPF algorithms, while maintaining the accuracy and reducing the size of a full representation approach; and 2) it conducts a comparative analysis of how load modeling influences the cost of ensuring stability and provides a summary of several recommendations for load modeling in these algorithms. The results show that the usual approach in TSCOPF studies, which involves impedance-based load modeling, leads to a significant false stabilization effect in the rotor angle trajectories. On the other hand, the use of the constant power model yields conservative results at a significant computational cost. This paper advocates for the adoption of the relevant node TSCOPF approach proposed in this work, retaining detailed exponential or polynomial load models for their flexibility and accuracy, while incurring only a slight increase in the computational effort.

INDEX TERMS Non-linear programming, optimal power flow, power system transient stability, TSCOPF.

NOMENCLATURE

ABBREVIATIONS

AVR	Automatic Voltage Regulator.
COI	Center of Inertia.
ELM	Exponential load model.
GAMS	General Algebraic Modeling System.
IPOPT	Interior Point Optimizer.
OPF	Optimal Power Flow.
PLM	Polynomial load model.
PSS	Power System Stabilizer.
PSSE	Power System Simulator for Engineering.
TSCOPF	Transient Stability Constrained Optimal Power Flow.

INDICES AND SETS

i,j	Indices for nodes.
t	Index for time steps.
Ω^{N}	Set of nodes of the system.
Ω^{RN}	Set of nodes of the reduced equivalent system.
Ω^{G}	Set of generation units.
Ω^{T}	Set of all time steps.
Ω^{TF}	Set of fault time steps.

PARAMETERS

A^{G}, B^{G}, C^{G}	Fuel cost coefficients of the power plants [€/MWh^2, €/MWh, €].
D	Damping coefficient of a power plant [p.u.].
H	Inertia coefficient of a power plant [s].
K^{PV}, K^{QV}	Active and reactive power coefficients of the exponential load model.

The associate editor coordinating the review of this manuscript and approving it for publication was Arturo Conde.

K^{PF}, K^{QF}	Active and reactive power coefficients of the frequency dependency of load.
P^{LN}, Q^{LN}	Active and reactive nominal load [p.u.].
P^{MIN}, P^{MAX}	Active power limits of a power plant [p.u.].
P^{Z}, P^{I}, P^{P}	Active power coefficients of the polynomial load model.
Q^{MIN}, Q^{MAX}	Reactive power limits of a power plant [p.u.].
Q^{Z}, Q^{I}, Q^{P}	Reactive power coefficients of the polynomial load model.
U^{MIN}, U^{MAX}	Limits of the bus voltage [p.u.].
U^{CORR}	Reference voltage for disconnecting a load [p.u.].
$Y_{i,j}$	Absolute value of element (i,j) of the reduced system admittance matrix.
$Y^{FS}_{i,j}$	Absolute value of element (i,j) of the full system admittance matrix.
X^{D}	Transient reactance of a power plant [p.u.].
ΔT	Integration time step [s].
$\Delta\omega^{MIN}$, $\Delta\omega^{MAX}$	Limits of the speed deviation of a synchronous power plant [p.u.].
$\theta_{i,j}$	Phase of the element (i,j) of the reduced system admittance matrix.
$\theta^{FS}_{i,j}$	Phase of the element (i,j) of the full system admittance matrix.
δ^{MAX}	Limit of the rotor angle deviation for a synchronous power plant [rad].
ω^{o}	Grid reference frequency [rad/s].

VARIABLES

e	Internal voltage of a synchronous power plant [p.u.].
f^{LV}	Binary factor that disconnects a load if the voltage drops below a reference.
p^{E}	Electrical power output at the rotor of a power plant [p.u.].
p^{G}, q^{G}	Active and reactive power output of a power plant [p.u.].
p^{L}, q^{L}	Active and reactive power consumption of a load
u	Bus voltage magnitude [p.u.].
α	Phase of the bus voltage [rad].
Δf^{COI}	Speed deviation of the center of inertia [p.u.].
$\Delta\omega$	Rotor speed deviation of a synchronous power plant [p.u.].
δ	Rotor angle of a synchronous power plant [rad].
δ^{COI}	Rotor angle of the center of inertia [rad].

I. INTRODUCTION

Transient Stability Constrained Optimal Power Flow (TSCOPF) models emerged two decades ago as a useful tool for the operation and planning of power systems [1], [2], [3]. These algorithms have recently gained attention [4], [5], [6], [7], [8], [9], [10] owing to advances in optimization algorithms and the challenges facing modern power systems in the transition toward decarbonization.

TSCOPF models combine an OPF formulation with transient stability constraints to ensure both economic operation and a transiently stable solution under a set of severe incidents. The inclusion of static and dynamic constraints in a single optimization model becomes challenging for a number of different reasons: the size of the problem, its non-linear nature, and the complexity of the static and dynamic power system models. Several approaches are proposed in the literature, to solve TSCOPF formulations [11]: 1) Simultaneous discretization techniques; 2) Simplification-based techniques; and 3) Metaheuristic optimization techniques. References [10] and [11] provide an extensive and comprehensive review, summarizing the different approaches to solving TSCOPF formulations. Simultaneous discretization methods have the advantage of including the dynamics of all power plants and using standard non-linear programming solvers in economic and security optimization. The two main drawbacks of simultaneous discretization are the large number of constraints and variables and the high non-linearity of the electromechanical oscillations between synchronous power plants, which creates large non-linear optimization problems that are difficult to solve.

The conventional practice in TSCOPF algorithms is to model loads using constant impedances. The use of different load models poses a challenge in these formulations because of the complexity of integrating them into the system of differential-algebraic equations that model the dynamic response of the system, included all together as constraints in the optimization problem. Transient stability studies based on time-domain simulation often do not model the entire transmission system during and after a fault. Instead, they convert the loads into shunt-connected impedances, incorporating them into the admittance matrix and then applying the Kron method to reduce the size of the model and the computational burden [13]. The Kron reduction produces an equivalent linear system with as many electrical nodes as connected synchronous power plants [14]. Most of the TSCOPF algorithms proposed in the literature, based on the direct discretization technique, follow this approach by modeling only the time-domain response of the synchronous power plants to evaluate transient stability. The result is an optimization model that can be solved with less computational effort; however, the load model skews the solution from the real one because load modeling significantly impacts dynamic simulations [12], [13], and this effect is not properly accounted for. This was particularly remarked on [17], where the reported TSCOPF solutions were re-evaluated using the equal-area criterion and trajectory sensitivity analysis. From these results, [17] affirmed that reported TSCOPF solutions are not viable if detailed load models are not considered, concluding that future efforts should be made to propose a robust

TSCOPF algorithm that allows the inclusion of detailed load models.

Following this path, this paper proposes a robust TSCOPF formulation based on a relevant node representation approach that allows the representation of any kind of detailed load model, while reducing the size of a full system representation. Besides generation buses, the buses with non-linear loads are also kept in the Kron reduction in fault and post-fault periods, maintaining the balance between an adequate representation of the system and the computational effort. The proposed model incorporates the most widely used load models in the industry [18] to conduct a comparative analysis of the influence of load modeling on transient stability and power generation cost. The proposed TSCOPF model has been successfully validated against time-domain simulations in PSSE.

The modeling of loads in transient stability simulations is challenging because a typical load is composed of several devices with different electrical equivalents. Even if the composition of the load is known in detail, it is not practical to represent each individual component at the transmission level, as there may be a large number of them, and they also change over time [19]. Consequently, it is standard practice (both in academia and industry) to use aggregate load models [16], [18], [20], [21]. Although all types of load models can be used in the proposed algorithm, this paper focuses on the most frequently used and those for which parameters are found in the available literature. According to [22], 74% of the surveyed TSOs and utilities use exponential and polynomial load models for dynamic power system analysis. The main contributions of this paper are:

- A robust TSCOPF formulation that accommodates any type of load model, based on the relevant node representation approach proposed in this study. The algorithm improves the performance of full system representation formulations while maintaining the same accuracy of results.
- A comprehensive and critical analysis of how load modeling influences the dispatch and the cost of energy generation provided by TSCOPF algorithms. This analysis encompasses the examination of the five most widely used load models in the industry.
- Several recommendations, drawn from the insights gained through this research, for integrating suitable load models into TSCOPF algorithms.

The proposed formulation has been implemented using a flexible computational framework based on MATLAB-GAMS that facilitates its application to different power systems. The optimization problem is solved in GAMS using the interior point-based optimization library IPOPT. The proposed formulation is tested on the Anderson IEEE 9, New England IEEE 39, and IEEE118 benchmark systems.

The rest of the paper is organized as follows: Section II describes the proposed optimization model; Section IV describes the implementation and validation of the proposed tool; Section V presents and discusses the results; and Section V concludes the paper.

II. OPTIMIZATION MODEL

This section describes the TSCOPF formulation based on the relevant node representation approach proposed in this work. The formulation makes it possible to represent any kind of detailed load model, including those that are dependent on the bus voltage and the system frequency in the time-domain. Section II-A presents the mathematical formulation of the TSCOPF algorithm; Section II-B describes the formulation to include the load models studied in this work corresponding to those most used in the industry.

A. TSCOPF MODEL

The proposed method combines the steady state representation with the dynamic response of the power system.

The optimization model is as follows:

$$\min f\left(p^{\mathrm{G}}_{i,1}\right) = \sum_{i=1}^{\mathrm{G}} \mathrm{A}^{\mathrm{G}}_i p^{\mathrm{G}^2}_{i,1} + \mathrm{B}^{\mathrm{G}}_i p^{\mathrm{G}}_{i,1} + \mathrm{C}^{\mathrm{G}}_i \tag{1}$$

Subject to:

$$p^{\mathrm{G}}_{i,1} - \mathrm{P}^{\mathrm{LN}}_i = u_{i,1} \sum_{j=1}^{\mathrm{N}} u_{j,1} \mathrm{Y}^{\mathrm{FS}}_{i,j} \cos\left(\alpha_{i,1} - \alpha_{j,1} - \theta^{\mathrm{FS}}_{i,j}\right), \quad \forall i \in \Omega^{\mathrm{N}} \tag{2}$$

$$q^{\mathrm{G}}_{i,1} - \mathrm{Q}^{\mathrm{LN}}_i = u_{i,1} \sum_{j=1}^{\mathrm{N}} u_{j,1} \mathrm{Y}^{\mathrm{FS}}_{i,j} \sin\left(\alpha_{i,1} - \alpha_{j,1} - \theta^{\mathrm{FS}}_{i,j}\right), \quad \forall i \in \Omega^{\mathrm{N}} \tag{3}$$

$$\mathrm{U}^{\mathrm{MIN}}_i \le u_{i,1} \le \mathrm{U}^{\mathrm{MAX}}_i, \forall i \in \Omega^{\mathrm{N}} \tag{4}$$

$$\mathrm{P}^{\mathrm{MIN}}_i \le p^{\mathrm{G}}_{i,1} \le \mathrm{P}^{\mathrm{MAX}}_i, \forall i \in \Omega^{\mathrm{G}} \tag{5}$$

$$\mathrm{Q}^{\mathrm{MIN}}_i \le q^{\mathrm{G}}_{i,1} \le \mathrm{Q}^{\mathrm{MAX}}_i, \forall i \in \Omega^{\mathrm{G}} \tag{6}$$

$$\alpha_{1,1} = 0 \tag{7}$$

$$p^{\mathrm{G}}_{i,1} \mathrm{X}^{\mathrm{D}}_i = e_i u_{i,1} \sin\left(\delta_{i,1} - \alpha_{i,1}\right), \forall i \in \Omega^{\mathrm{G}} \tag{8}$$

$$q^{\mathrm{G}}_{i,1} \mathrm{X}^{\mathrm{D}}_i = e_i u_{i,1} \cos\left(\delta_{i,1} - \alpha_{i,1}\right) - u^2_{i,1}, \forall i \in \Omega^{\mathrm{G}} \tag{9}$$

$$\Delta\omega_{i,1} = 0, \forall i \in \Omega^{\mathrm{G}} \tag{10}$$

$$p^{\mathrm{G}}_{i,1} = p^{\mathrm{E}}_{i,1}, \forall i \in \Omega^{\mathrm{G}} \tag{11}$$

$$\delta_{i,t} - \delta_{i,t-1} - \left(\Delta T \frac{\omega^0}{2}\right)\left(\Delta\omega_{i,t} + \Delta\omega_{i,t-1}\right) = 0, \forall i \in \Omega^{\mathrm{G}}, t = 2 \ldots \mathrm{T} \tag{12}$$

$$\Delta\omega_{i,t}\left(1 + \Delta\mathrm{TD}_i/(4\mathrm{H}_i)\right) - \Delta\omega_{i,t-1} \times \left(1 - \Delta\mathrm{TD}_i/(4\mathrm{H}_i)\right) - \left(\Delta T/(4\mathrm{H}_i)\right) \times \left(2p^{\mathrm{G}}_{i,1} - p^{\mathrm{E}}_{i,t} - p^{\mathrm{E}}_{i,t-1}\right) = 0, \forall i \in \Omega^{\mathrm{G}}, t = 2 \ldots \mathrm{T} \tag{13}$$

$$p^{\mathrm{E}}_{i,t} \mathrm{X}^{\mathrm{D}}_i = e_i u_{i,t} \sin\left(\delta_{i,t} - \alpha_{i,t}\right), \forall i \in \Omega^{\mathrm{G}}, t = 2 \ldots \mathrm{T} \tag{14}$$

$$(e_i u_{i,t}\sin(\delta_{i,t}-\alpha_{i,t}))/\mathrm{X}_i^{\mathrm{D}} - p_{i,t}^{\mathrm{L}} = u_{i,t}\sum_{j=1}^{\mathrm{RN}} u_{j,t}\mathrm{Y}_{i,j,t}\cos\left(\alpha_{i,t}-\alpha_{j,t}-\theta_{i,j,t}\right), \quad \forall i\in\Omega^{\mathrm{RN}}, t=2\ldots\mathrm{T} \tag{15}$$

$$(e_i u_{i,t}\cos(\delta_{i,t}-\alpha_{i,t}) - u_{i,t}^2)/\mathrm{X}_i^{\mathrm{D}} - q_{i,t}^{\mathrm{L}} = u_{i,t}\sum_{j=1}^{\mathrm{RN}} u_{j,t}\mathrm{Y}_{i,j,t}\sin\left(\alpha_{i,t}-\alpha_{j,t}-\theta_{i,j,t}\right), \quad \forall i\in\Omega^{\mathrm{RN}}, t=2\ldots\mathrm{T} \tag{16}$$

$$\delta_t^{\mathrm{COI}} = (\sum_{i=1}^{\mathrm{G}}\mathrm{H}_i\delta_{i,t})/(\sum_{i=1}^{\mathrm{G}}\mathrm{H}_i), \forall t\in\Omega^{\mathrm{T}} \tag{17}$$

$$-\delta^{\mathrm{MAX}} \le \delta_{i,t}-\delta_t^{\mathrm{COI}} \le \delta^{\mathrm{MAX}}, \forall i\in\Omega^{\mathrm{G}}, t=2\ldots\mathrm{T} \tag{18}$$

$$\Delta\omega_{i,t}^{\mathrm{MIN}} \le \Delta\omega_{i,t} \le \Delta\omega_{i,t}^{\mathrm{MAX}}, \forall i\in\Omega^{\mathrm{G}}, t=2\ldots\mathrm{T} \tag{19}$$

The model defined by (1)-(19) combines an Optimal Power Flow (OPF) model (1)-(7) with the constraints to include the time-domain representation of the system under one or more contingencies (8)-(16) and the transient and frequency stability limits (17)-(19) in the optimization problem. The objective function (1) minimizes the power generation cost of the system as a quadratic function. Constraints (2) and (3) are the load flow at each bus of the system during the steady-state operation. Inequality constraints (4), (5), and (6) represent the voltage limits at each node of the system, and the active and reactive power generation limits of the power plants, respectively. Constraint (7) sets the angle reference in the slack node.

In this work, power plants are modeled using the classical synchronous generator model, composed of a voltage source behind a transient reactance [19]. However, more detailed representations of the generators can easily be included [7] including Automatic Voltage Regulators (AVR), Turbine Governors, and Power System Stabilizers (PSS) [23]. Constraints (8) and (9) relate the internal variables of the synchronous generators to the variables at the connecting bus and initialize the internal variables of the power plants for the time-domain simulation. The differential equations that model the dynamic response of the system, under one or more contingencies, are discretized using the trapezoidal rule and included as constraints of the non-linear optimization problem. Constraints (10)-(13) model the swing equation of synchronous power plants through two separate differential equations (20)-(21): one for the rotor angle deviation (20) and one for the rotor speed deviation (21). Constraints (10)-(11) correspond to the initialization of the time-domain simulation. Constraints (12)-(13) calculate the rotor angle and rotor speed deviation at every time step of the fault and post-fault periods, and are obtained by applying the trapezoidal rule to differential equations (20)-(21). Constraint (14) calculates the electrical power injected by the synchronous power plants during the time-domain simulation.

$$\frac{d\delta}{dt} = \omega^o\Delta\omega \tag{20}$$

$$\frac{d\Delta\omega}{dt} = \frac{1}{2\mathrm{H}}(p^{\mathrm{M}} - p^{\mathrm{E}} - D\Delta\omega) \tag{21}$$

For the time-domain simulation (fault and post-fault periods), an equivalent system is calculated and represented by the admittance matrix $Y\perp\theta$, removing all transmission buses from the full system admittance matrix $Y^{\mathrm{FS}}\perp\theta^{\mathrm{FS}}$ by the Kron reduction method [21], but maintaining all nodes where power plants, non-linear loads, and/or other relevant devices are connected. Consequently, the response of all active elements and the non-linearity of loads are preserved during the time-domain representation while reducing the size of the optimization problem. Constraints (15)-(16) calculate the load flow equations at the buses of the admittance matrix $Y\perp\theta$, where active or passive non-linear elements are connected during each time step. The admittance matrix $Y\perp\theta$ changes in fault and post-fault periods to model the studied contingency. Typical contingencies include short circuits followed by switching actions to clear the fault.

Transient and frequency stability constraints are both included in the proposed model (17)-(19). The transient stability constraint (18) is represented as a limit on the deviation of the rotor angles of the synchronous power plants, with respect to the center of inertia (COI) calculated in (17). The frequency stability limit is implemented as a maximum deviation on the rotor speed of the synchronous power plants (19).

B. LOAD MODELING

Load modeling has a significant impact on the results of transient stability and must, therefore, be properly accounted for in TSCOPF models. The usual practice in direct discretization TSCOPF models is to represent loads as constant impedances, to include them within the admittance matrix and then apply the Kron reduction method to obtain an equivalent system with only the generation buses [11]. The results obtained using these models must be treated with caution because modeling loads using a constant impedance mitigates the rotor angle and rotor speed deviations over real trajectories and can provide solutions that, in real systems, are unstable [24]. Figure 1 illustrates the most used load models in power system studies, according to a survey conducted by the Working Group C4.605: "Modeling and aggregation of loads in flexible power networks" to more than 160 utilities and system operators in over 50 countries on five continents in [22].

The TSCOPF model defined by (1)-(19) is completed with the following equations that represent the main load models used in industry, according to [20], but any other type of load model can also be included.

C. EXPONENTIAL LOAD MODEL

Equations (22)-(23) represent the exponential load model for active and reactive power in the proposed TSCOPF.

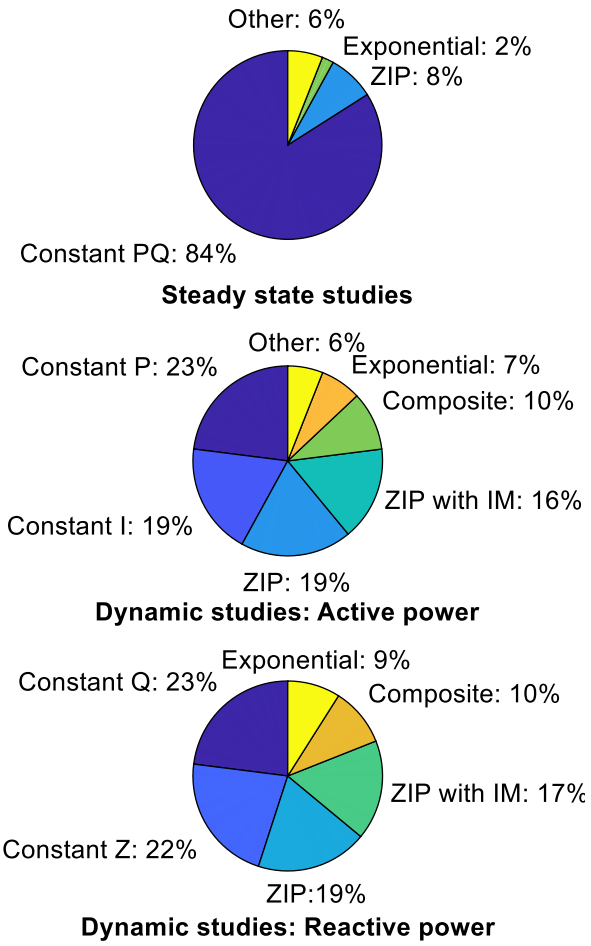

FIGURE 1. Load models used in industry according to the survey elaborated by the working group C4.605 in [22].

For voltage exponent values K^{PV} and K^{QV} equal to 0, 1 and 2, this load model represents constant power, constant current, and constant impedance loads, respectively. The frequency dependency of loads is represented by multiplying the exponential load model by the factor $(1+K^{PF}\Delta f_t^{COI})$, where Δf_t^{COI} is the frequency deviation of the center of inertia.

$$p_{i,t}^{L} = P_i^{LN}\left(\frac{u_{i,t}}{u_{i,1}}\right)^{K^{PV}}(1+K^{PF}\Delta f_t^{COI}),\ \forall i\in\Omega^{RN},\ t=2\ldots T \tag{22}$$

$$q_{i,t}^{L} = Q_i^{LN}\left(\frac{u_{i,t}}{u_{i,1}}\right)^{K^{QV}}(1+K^{QF}\Delta f_t^{COI}),\ \forall i\in\Omega^{RN},\ t=2\ldots T \tag{23}$$

D. POLYNOMIAL LOAD MODEL

Equations (24)-(25) represent the polynomial (also known as ZIP) load model for active and reactive power in the proposed TSCOPF. This model is composed of constant impedance, constant current, and constant power components. Parameters P^Z, P^I, and P^P determine the proportion of each for the active power component, and Q^Z, Q^I, and Q^P determine the proportion for the reactive power component. Their sum equals 1. The frequency dependency of the load is also represented by multiplying the polynomial load model by the factor $(1+K^{PF}\Delta f_t^{COI})$.

$$p_{i,t}^{L} = P_i^{LN}\left[P^Z\left(\frac{u_{i,t}}{u_{i,1}}\right)^2 + P^I\left(\frac{u_{i,t}}{u_{i,1}}\right) + P^P\right] \times\left(1+K^{PF}\Delta f_t^{COI}\right),\ \forall i\in\Omega^{RN},\ t=2\ldots T \tag{24}$$

$$q_{i,t}^{L} = Q_i^{LN}\left[Q^Z\left(\frac{u_{i,t}}{u_{i,1}}\right)^2 + Q^I\left(\frac{u_{i,t}}{u_{i,1}}\right) + Q^P\right] \times\left(1+K^{QF}\Delta f_t^{COI}\right),\ \forall i\in\Omega^{RN},\ t=2\ldots T \tag{25}$$

E. FREQUENCY DEVIATION OF THE CENTER OF INERTIA

For the frequency dependence component in both the exponential and polynomial load models, constraint (26) is also included in the proposed TSCOPF (1)-(19) to calculate the system frequency deviation of the Center of Inertia (COI) in each period of time.

$$\Delta f_t^{COI} = \frac{\sum_{i=1}^{N} H_i\Delta\omega_{i,t}}{\sum_{i=1}^{N} H_i},\ \forall t\in\Omega^{T} \tag{26}$$

In both exponential and polynomial models, the frequency dependence can be neglected by setting the K^{PF} and K^{QF} parameters equal to 0, as is often considered in the industry [21].

F. MODELING LOADS DURING VOLTAGE DIPS

During faults provoking very low voltages, the model can suffer from numerical instability if the constant power component is dominant. This component would introduce a constant value into the power flow equations (15)-(16), that would make them mathematically inconsistent when a short circuit occurs, provoking the voltage values at a load bus being close to zero. To handle this issue, the additional constraint (27) can be included in the optimization model to reduce the power consumption when the voltage at the connecting point reaches very low values. Constraint (27) calculates $f_{i,t}^{LV}$ factor for all buses and all time steps, taking the value 1 when the voltage does not fall below U^{CORR} (in this work 0.2 p.u.), and quadratically decreases toward 0 when the voltage is lower. Then, this factor is introduced as a product in the constraints (22)-(23) or (24)-(25), depending on the chosen load model, during the fault stage.

$$f_{i,t}^{LV} = \min\left[1, \left(\frac{u_{i,t}^2}{U^{CORR^2}}\right)\right],\ \forall i\in\Omega^{RN},\ \forall t\in\Omega^{TF} \tag{27}$$

When constraint (27) is included in the optimization problem, it changes from a non-linear optimization problem (NLP) to a non-linear optimization problem with discontinuous derivatives (DNLP). The inclusion of this restriction significantly affects the computation time, and this effect is discussed in Section V.

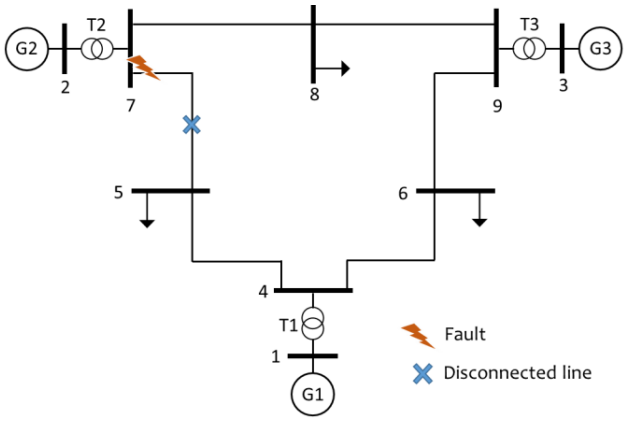

FIGURE 2. Anderson IEEE9 bus test system and fault location.

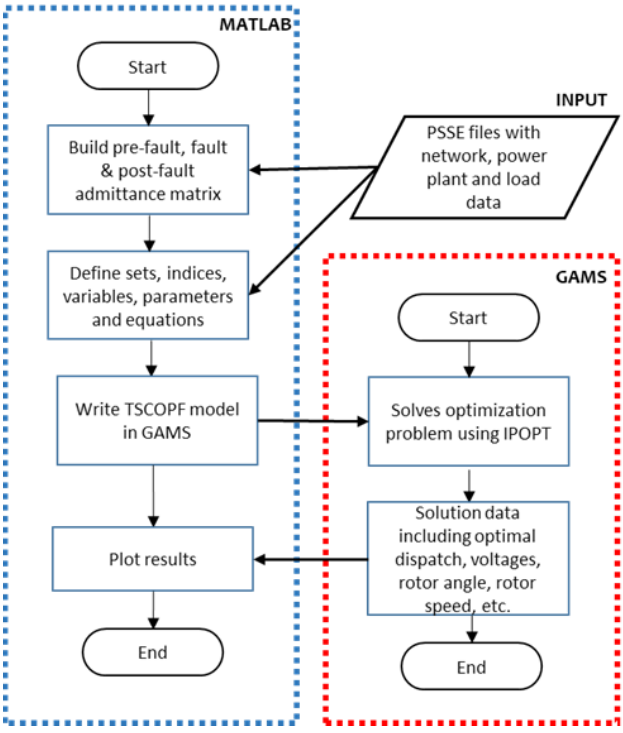

FIGURE 3. Software implementation for TSCOPF.

III. IMPLEMENTATION AND VALIDATION

Figure 3 illustrates the software framework used to build and solve the optimization problem which is described as follows:

1. A program written in MATLAB reads the data corresponding to the network, power plants and loads from standard PSSE files. The information on critical contingencies and switching actions is introduced, and the program automatically builds the full system admittance matrices $\mathrm{Y}_{i,t}^{\mathrm{FS}} \perp \theta_{i,t}^{\mathrm{FS}}$ for the pre-fault, fault, and post-fault periods of the simulation.
2. The program searches for transmission nodes where no elements are connected and eliminates these nodes in the fault and post-fault admittance matrices by applying the Kron reduction method. The result is a reduced equivalent network which includes the buses where power plants, loads or other elements are connected, represented by the admittance matrices $\mathrm{Y}_{i,t} \perp \theta_{i,t}$ for those periods.
3. The program calls GAMS through the GDXMRW routine [25] and solves the optimization problem using the interior point library IPOPT [25], which solves large-scale non-linear optimization problems using a prime-dual interior point method.
4. Finally, when the routine finishes, it returns the solution to MATLAB for data analysis and plotting.

This approach facilitates the application of the optimization model to different electric power systems and allows the user to easily modify the network topology, the load, the contingencies, and the optimization solver.

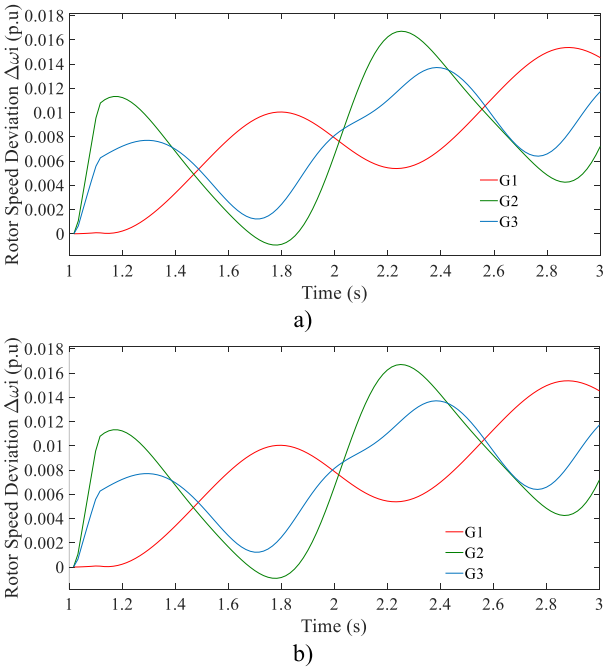

FIGURE 4. TSCOPF model validation when a three phase short-circuit occurring near bus 7 at the end of line 5-7. The fault is cleared after 5 cycles (0.083s) by opening line 5-7. a) Rotor speed deviation of the synchronous power plants obtained after the solution of the optimization model in GAMS; b) Validation of the result using PSSE.

Figure 4 presents an example of validation for the proposed algorithm applied to the Anderson IEEE 9 bus test system (Figure 2). All system data can be found in [14]. The simulated fault is a three-phase short-circuit that occurs near bus 7, at the end of line 5-7, and is cleared after 5 cycles (0.083s) by opening line 5-7. Figure 4.a shows the rotor speed deviations obtained by the TSCOPF algorithm in synchronous power plants. Figure 4.b shows the same variables using PSSE.

IV. RESULTS AND DISCUSSION

A. PERFORMANCE OF THE PROPOSED TSCOPF IMPLEMENTATION

This section presents a comparative analysis of the size and computational burden of the following TSCOPF models:

TABLE 1. Comparison between the three different approaches applied to the Anderson ieee 9 benchmark test system.

Algorithm	Does it allow detailed load modeling?	Number of constraints/variables	Convergence time (s)
Reduced system approach	No	1223/1221	0.350
Full system representation approach	Yes	3365/3363	0.900
Relevant node representation approach	Yes	2651/2649	0.549

TABLE 2. Comparison between the three different approaches applied to the new England ieee 39 benchmark test system.

Algorithm	Does it allow detailed load modeling?	Number of constraints/variables	Convergence time (s)
Reduced system approach	No	3827/3808	7.5
Full system representation approach	Yes	13109/13090	16.3
Relevant node representation approach	Yes	10253/10234	10.2

TABLE 3. Comparison between the three different approaches applied to the IEEE118 benchmark test system.

Algorithm	Does it allow detailed load modeling?	Number of constraints/variables	Convergence time (s)
Reduced system approach	No	7615/7576	27.3
Full system representation approach	Yes	42613/42101	55.5
Relevant node representation approach	Yes	37856/37422	43.3

- Reduced system approach [11]: This implementation is currently the most widespread in TSCOPF. All the loads are represented as impedances in the admittance matrix, and the system is reduced to represent only the response of the synchronous power plants during the time-domain simulation.
- Full system representation approach [7], [26]: The time-domain simulation includes the representation of all the nodes in the system at all time steps, making it possible to model non-linear loads.
- Relevant node representation approach: This corresponds to the implementation proposed in this work, in which the system is reduced but removes only those nodes where no active elements are connected. This proposal presents the advantages of the full system representation approach while reducing the size of the optimization problem.

Table 1, Table 2, and Table 3 present the results obtained using the three different approaches when applied to various IEEE Benchmark systems: 1) the Anderson IEEE 9 system, which includes 9 buses and 3 power plants [14]; 2) the New England IEEE 39 system, comprising 39 buses and 10 power plants [27]; and 3) the IEEE118 system, which includes 20 power plants and 118 buses [27]. The dynamic data for the three systems can be found in [14], [28], and [29], respectively. The following contingencies are represented in each system with an integration time step of 0.01667s: 1) a three-phase short-circuit at the transmission line connecting buses 7 and 5, adjacent to bus 7 and cleared by opening the circuit breakers at the two ends of the line after 0.08335 s; and 2) a three-phase short-circuit at the transmission line connecting buses 3 and 4, adjacent to bus 3 and cleared by opening the circuit breakers at the two ends of this line after 0.08335 s; and 3) a three-phase short-circuit at the transmission line connecting buses 65 and 68, adjacent to bus 65 and cleared by opening the circuit breakers at the two ends of this line after 0.08335 s. In all the case studies presented in the paper, voltage limits (U_i^{MIN} and U_i^{MAX}) are set at 0.95 p.u. and 1.05 p.u. The maximum deviation on the rotor angle (δ^{MAX}) is defined as 60 degrees. The frequency stability limits ($\Delta\omega_{i,t}^{MIN}$ and $\Delta\omega_{i,t}^{MAX}$) are -0.02 p.u. and 0.02 p.u., respectively.

The results show that for the standard implementation in the literature (presented here as the Reduced System Approach), the size of the optimization problem, both in terms of the number of constraints and variables, is smaller in comparison with the full system and the relevant node representation approaches and, consequently, the convergence time is also faster. However, this approach does not consider the influence of the dynamics of elements such as non-linear loads, non-synchronous renewable generation, or energy storage systems, and might not be suitable for applications in modern electrical power systems, where these devices play an increasingly important role. The full system representation approach, first proposed in [30], solves this challenge but at the expense of a considerable increase in the size of the optimization problem and the convergence times, as shown for the different case studies in Table 1, Table 2, and Table 3.

The relevant node representation approach proposed in this work aims to reduce the size of the problem and convergence times, while maintaining the advantages of the full system representation approach. The results presented clearly indicate that the relevant node representation algorithm achieves its objectives, since there is a significant reduction in the number of constraints and variables and, even further, in the convergence time for all case studies.

B. EFFECT OF LOAD MODELING ON TRANSIENT STABILITY AND POWER GENERATION COST

This section presents a comparative analysis of the influence of load modeling on the transient stability and power

TABLE 4. TSCOPF results when using different load models applied to the Anderson IEEE 9 bus test system.

Power plant data						
Marginal cost ($/MWh)	59	31	22	**Convergence time (s)**	**Cost ($)**	**ΔCost (%)**
Nominal power (MW)	300	200	150			
Power plant	**G1 (MW)**	**G2 (MW)**	**G3 (MW)**			
OPF Results	-	174	150	0.192	8689	-
TSCOPF Results						
Constant Impedance (Z)	46	125	150	0.829	9886	13.8%
Constant Current (I)	49	122	150	0.800	9960	14.6%
Constant Power (P)	67	103	150	**12.530**	10433	20%
Exponential load model (ELM)	55	116	150	0.822	10115	16.4%
Polynomial load model (PLM)	54	117	150	0.816	10084	16%

generation cost for TSCOPF studies. The study is carried out using the optimization model based on the relevant node representation approach proposed in this work, which allows the use of any type of load model. Section II provides an explanation of the standard load models commonly used in the industry and their corresponding equations within the TSCOPF. This section analyzes the impact of the following five load models, which are among the most commonly used: 1) Constant impedance (Z) using (22) and (23) with parameters K^{PV} and K^{QV} equal to 2; 2) Constant current (I) using (22) and (23) with K^{PV} and K^{QV} equal to 1; 3) Constant power (P) using (22)-(23) and (27) with parameters K^{PV} and K^{QV} equal to 0; 4) Exponential load model (ELM) using (22)-(23) with parameters K^{PV} and K^{QV} equal to 0.56 and 1.21, respectively, which are taken from [21]; and 5) Polynomial load model (PLM) using (24) and (25) considering a mixed load of 20% constant impedance (with parameters P^Z, Q^Z equal to 0.2), 20% constant current (with parameters P^I, Q^I equal to 0.2), and 60% constant power (with parameters P^P, Q^P equal to 0.6). Initially, the load frequency dependence characteristic was neglected, considering K^{PF} and K^{QF} to be equal to 0 for all cases, which is a common practice in the industry [15].

Table 4 presents the results obtained using the five different load models for TSCOPF and compares them to those obtained using an Optimal Power Flow (OPF) algorithm. For the sake of clarity, the results are presented for the Anderson IEEE 9 bus system and the same contingency described in the previous section.

The solution for a classical OPF results in a generation cost of 8689 €, with G2 generating 174 MW and G3 generating 150 MW (full load), as shown in the OPF row of Table 4. The application of the TSCOPF model, which takes into account the stability limits, indicates that the result given by the OPF is not stable under the considered contingency. The TSCOPF model increases the power generation cost, with respect to the OPF, because the algorithm shifts power from generator G2 to (the most expensive) G1, to ensure stability. This shows that dynamic constraints play a significant role because they affect the optimal dispatch. In other words, the solution provided by a classical OPF is not transiently stable and the TSCOPF modifies the dispatch, to ensure that the solution is stable.

Table 4 shows that, for the same case study, the TSCOPF presents significantly different results when using different load models. The most economical solution is given by the constant impedance load model, which is the standard in direct discretization TSCOPF algorithms. Impedance-based load models exhibit a quadratic reduction in power consumption when voltage drops due to a short circuit. This effect creates a false stabilizing impact as it reduces the difference between mechanical and electrical power in the swing equation (13), consequently mitigating rotor angle and rotor speed deviations along their real trajectories. This effect is shown in Figure 5 and Figure 6, where the rotor angle and rotor speed trajectories for power plant G2 are represented for the five case studies.

The solution obtained when using the exponential and polynomial load models provides the most accurate representation because they were set up using parameters obtained from aggregating the real loads. In these cases, the power dispatch changes significantly and increases the total generation cost compared to the solution obtained when using constant impedance or constant current models. The highest cost is reached when loads are modeled as a constant power, which could be considered the most conservative approach. It must be pointed out that the convergence time, in this case, increases significantly compared to other approaches. This is probably due to the binary constraint (27) introduced in a non-linear programming (NLP) algorithm to ensure mathematical stability.

Figure 5 and Figure 6 depict the rotor speed of power plant G2, obtained from the solution of the TSCOPF, for five different load models. Figure 5 shows the evolution over

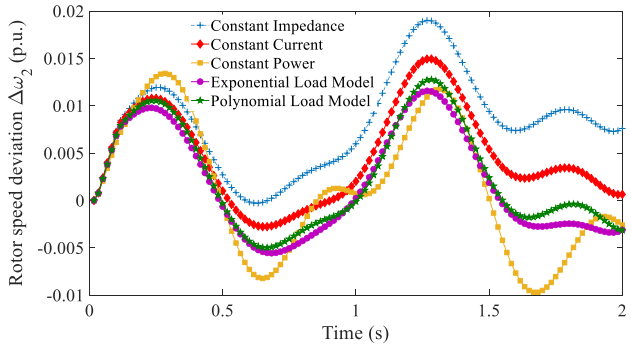

FIGURE 5. Rotor speed deviation of power plant G2 when using different load models.

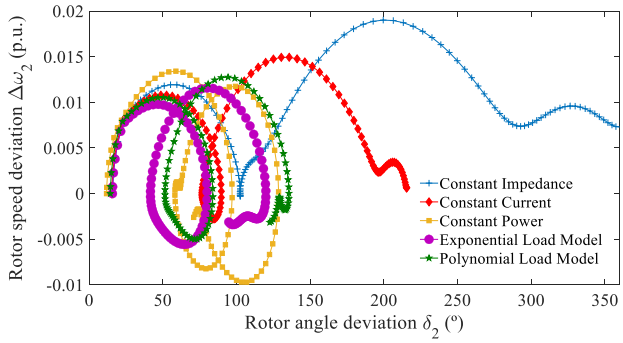

FIGURE 6. Rotor angle vs rotor speed deviation of power plant G2 when using different load models.

time, which allows a clear comparison between cases, while Figure 6 shows the rotor speed against rotor angle, which facilitates an assessment of the electro-mechanical oscillations. It can be seen that:

- The detailed exponential and polynomial load models exhibit similar trajectories and can be taken as a reference.
- The solution obtained with the constant current load is not very different from the detailed load models, which explains why its generation cost in Table 4 is also similar. This result is consistent with the recommendation given in [31] that, in the absence of detailed information on the composition of loads, real power demand can be represented using a constant current.
- The trajectory resulting from the constant impedance load exhibits the most damped oscillations, leading to the lowest generation cost in Table 4. Nonetheless, it is also the least conservative of the five, raising concerns about real-life stability. The use of a constant impedance load model may lead to potentially unstable solutions.
- The trajectory associated with the constant power load model shows the largest electromechanical oscillations, consequently leading to the highest generation cost in Table 4.

It must be stressed that, for other case studies solved in the Anderson IEEE 9 and in the other larger test systems, the variables and economic results follow the same trend, providing the same conclusions.

TABLE 5. Tscopf results considering the frequency dependence of load.

Frequency Dependence of Load	G1 (MW)	G2 (MW)	G3 (MW)	Conv. time (s)	Cost (€)
		Exponential load model			
Neglected	54.39	116.3	150	0.822	10114.31
Included	54.22	116.5	150	0.941	10110.48
		Polynomial load model			
Neglected	53.4	117.2	150	0.816	10083.8
Included	53	117.6	150	0.792	10072.6

C. INFLUENCE OF THE FREQUENCY DEPENDENCY OF LOAD

The frequency dependency of load is often neglected in time-domain transient stability studies [15]. This section conducts an in-depth analysis to evaluate both the computational burden associated with accounting for this effect and the quantitative impact on the economic and power dispatch results as provided by TSCOPF when considering or neglecting it. In the proposed optimization model, this effect is considered by including values for the parameters K^{PF} and K^{QF} in constraints (22)-(23), for the exponential load model, and in (24)-(25), for the polynomial load model. These parameters are different for each electrical system and, for different operating point and depend on the type of load connected in each period of time. In this section, general values for K^{PF} (0.69) and K^{QF} (−8.89) are considered, which are taken from [21]. Table 5 shows the results obtained when including the frequency dependency of load in TSCOPF. The results are slightly different, in terms of generation cost and convergence time, in comparison to those obtained when neglecting this effect. For all studied cases, this load characteristic provides a stabilizing effect to the system because the load increases when the frequency deviation is positive and vice versa, explaining the more economical results when accounting for the frequency dependency of load.

Regarding computational effort, the results in Table 5 suggest that including the frequency dependency of load in TSCOPF studies yields more accurate results while slightly affecting the computational times of the algorithm.

Based on the results obtained in several case studies, it has been observed that frequency dependency of load does not significantly impact the results. Therefore, it could be reasonable to neglect this effect, as the results provided by TSCOPF without considering it are more conservative.

V. CONCLUSION

This paper addresses the challenge posed in the literature concerning load models in TSCOPF studies. The results demonstrate the significant influence of load modeling on power dispatch and generation costs as provided by TSCOPF algorithms. Standard approaches based on modeling loads as impedances must be carefully reconsidered. In particular:

- Modeling loads as constant impedances leads to a false stabilization effect in simulations and, consequently,

provides the lowest generation cost. This representation is especially dangerous in TSCOPF algorithms because, as they search for the most economical solution, they provide results that are often close to the operational limits of the system. Consequently, the dispatch provided by a TSCOPF with constant impedance loads can result in unstable conditions during real operation.
- The use of a constant power model yields more conservative results, at higher costs; however, the studied cases show that the computational effort to solve the model increases dramatically because of the adjustments in the model which are needed to ensure convergence during voltage dips.
- The use of more detailed load models (both polynomial and exponential) slightly affects the convergence times, allowing the representation of real aggregate loads.
- Modeling the relation between load and frequency has only a minor effect on the results of the TSCOPF, generally stabilizing the system.

This paper proposes the application of exponential or polynomial load models to TSCOPF because their flexibility allows the representation of most kind of loads with accuracy and with a relatively slight increase in the computational effort. These models produced accurate results in the studied cases and have the advantage of being sanctioned by the industry, in conventional transient stability studies. They increase the complexity of the TSCOPF compared to the commonly used constant impedance model, but the increase in computational load is moderate and can be mitigated using the relevant node representation approach proposed in this paper. This approach removes the electrical nodes that do not connect to non-linear devices from the admittance matrix.

Future work is expected to encompass, but is not limited to, the following research directions: 1) Evaluating the performance of the proposed algorithm in open-source optimization software, such as Pyomo or Julia, in comparison to GAMS 2) Utilizing the software tool to optimize the operation of islanded power systems in the Spanish archipelagos. 3) Optimizing power plant control parameters using a modified version of the proposed tool; and 4) Collaborating with the system operator to conduct testing and further enhance the proposed software tool.

REFERENCES

[1] D. Gan, R. J. Thomas, and R. D. Zimmerman, "Stability-constrained optimal power flow," *IEEE Trans. Power Syst.*, vol. 15, no. 2, pp. 535–540, May 2000, doi: 10.1109/59.867137.

[2] Y. Yuan, J. Kubokawa, and H. Sasaki, "A solution of optimal power flow with multicontingency transient stability constraints," *IEEE Trans. Power Syst.*, vol. 18, no. 3, pp. 1094–1102, Aug. 2003, doi: 10.1109/tpwrs.2003.814856.

[3] M. La Scala, M. Trovato, and C. Antonelli, "On-line dynamic preventive control: An algorithm for transient security dispatch," *IEEE Trans. Power Syst.*, vol. 13, no. 2, pp. 601–610, May 1998, doi: 10.1109/59.667388.

[4] S. Xia, Z. Ding, M. Shahidehpour, K. W. Chan, S. Bu, and G. Li, "Transient stability-constrained optimal power flow calculation with extremely unstable conditions using energy sensitivity method," *IEEE Trans. Power Syst.*, vol. 36, no. 1, pp. 355–365, Jan. 2021, doi: 10.1109/TPWRS.2020.3003522.

[5] S. Hashemi, H. Lesani, and M. R. Aghamohammadi, "An integrated approach for incorporation of voltage and transient stabilities into optimal power flow study," *Electric Power Syst. Res.*, vol. 206, May 2022, Art. no. 107784, doi: 10.1016/j.epsr.2022.107784.

[6] X. Zhao, H. Wei, J. Qi, P. Li, and X. Bai, "Frequency stability constrained optimal power flow incorporating differential algebraic equations of governor dynamics," *IEEE Trans. Power Syst.*, vol. 36, no. 3, pp. 1666–1676, May 2021, doi: 10.1109/TPWRS.2020.3025335.

[7] F. Arredondo, P. Ledesma, E. D. Castronuovo, and M. Aghahassani, "Stability improvement of a transmission grid with high share of renewable energy using TSCOPF and inertia emulation," *IEEE Trans. Power Syst.*, vol. 37, no. 4, pp. 3230–3237, Jul. 2022, doi: 10.1109/TPWRS.2020.3022082.

[8] M. Aghahassani, E. D. Castronuovo, P. Ledesma, and F. Arredondo, "Evaluation of numerical methods for TSCOPF in a large interconnected system," *IEEE Access*, vol. 10, pp. 70562–70571, 2022, doi: 10.1109/ACCESS.2022.3187403.

[9] F. W. Liederer, J. C. López, M. J. Rider, and D. Dotta, "Transient stability constrained optimal power flow considering fourth-order synchronous generator model and controls," *Electric Power Syst. Res.*, vol. 213, Dec. 2022, Art. no. 108667, doi: 10.1016/j.epsr.2022.108667.

[10] S. Batchu and K. Teeparthi, "Transient stability enhancement through individual machine equal area criterion framework using an optimal power flow," *IEEE Access*, vol. 10, pp. 49433–49444, 2022, doi: 10.1109/ACCESS.2022.3173422.

[11] S. Abhyankar, G. Geng, M. Anitescu, X. Wang, and V. Dinavahi, "Solution techniques for transient stability-constrained optimal power flow—Part I," *IET Gener., Transmiss. Distribution*, vol. 11, no. 12, pp. 3177–3185, Aug. 2017, doi: 10.1049/iet-gtd.2017.0345.

[12] G. Geng, S. Abhyankar, X. Wang, and V. Dinavahi, "Solution techniques for transient stability-constrained optimal power flow—Part II," *IET Gener., Transmiss. Distribution*, vol. 11, no. 12, pp. 3186–3193, Aug. 2017, doi: 10.1049/iet-gtd.2017.0346.

[13] S. Ekinci, H. Lale Zeynelgil, and A. Demiroren, "A didactic procedure for transient stability simulation of a multi-machine power system utilizing SIMULINK," *Int. J. Electr. Eng. Educ.*, vol. 53, no. 1, pp. 54–71, Jan. 2016, doi: 10.1177/0020720915597935.

[14] P. M. Anderson and A. A. Fouad, *Power System Control and Stability*. Hoboken, NJ, USA: Wiley, 2008.

[15] Y. Zhu, J. V. Milanović, and K. N. Hasan, "Ranking and quantifying the effects of load model parameters on power system stability," *IET Gener., Transmiss. Distribution*, vol. 13, no. 20, pp. 4650–4658, Oct. 2019, doi: 10.1049/iet-gtd.2019.0489.

[16] Y. Zhu and J. V. Milanović, "Efficient identification of critical load model parameters affecting transient stability," *Electric Power Syst. Res.*, vol. 175, Oct. 2019, Art. no. 105929, doi: 10.1016/j.epsr.2019.105929.

[17] R. Zhang, Y. Xu, W. Zhang, Z. Y. Dong, and Y. Zheng, "Impact of dynamic load models on transient stability-constrained optimal power flow," in *Proc. IEEE PES Asia–Pacific Power Energy Eng. Conf. (APPEEC)*, Oct. 2016, pp. 18–23, doi: 10.1109/APPEEC.2016.7779462.

[18] A. Arif, Z. Wang, J. Wang, B. Mather, H. Bashualdo, and D. Zhao, "Load modeling—A review," *IEEE Trans. Smart Grid*, vol. 9, no. 6, pp. 5986–5999, Nov. 2018, doi: 10.1109/TSG.2017.2700436.

[19] P. Kundur, N. J. Balu, and M. G. Lauby, *Power System Stability and Control*. New York, NY, USA: McGraw-Hill, 1994.

[20] K. Yamashita, S. Djokic, J. Matevosyan, F. O. Resende, L. M. Korunovic, Z. Y. Dong, and J. V. Milanovic, "Modelling and aggregation of loads in flexible power networks—Scope and status of the work of CIGRE WG C4.605," *IFAC Proc. Volumes*, vol. 45, no. 21, pp. 405–410, Jan. 2012, doi: 10.3182/20120902-4-FR-2032.00072.

[21] L. M. Korunovic, J. V. Milanovic, S. Z. Djokic, K. Yamashita, S. M. Villanueva, and S. Sterpu, "Recommended parameter values and ranges of most frequently used static load models," *IEEE Trans. Power Syst.*, vol. 33, no. 6, pp. 5923–5934, Nov. 2018, doi: 10.1109/TPWRS.2018.2834725.

[22] J. V. Milanovic, K. Yamashita, S. M. Villanueva, S. Ž. Djokic, and L. M. Korunovic, "International industry practice on power system load modeling," *IEEE Trans. Power Syst.*, vol. 28, no. 3, pp. 3038–3046, Aug. 2013, doi: 10.1109/TPWRS.2012.2231969.

[23] V. Snášel, R. M. Rizk-Allah, D. Izci, and S. Ekinci, "Weighted mean of vectors optimization algorithm and its application in designing the power system stabilizer," *Appl. Soft Comput.*, vol. 136, Mar. 2023, Art. no. 110085, doi: 10.1016/j.asoc.2023.110085.

[24] A. Adrees and J. Milanović, "Effect of load models on angular and frequency stability of low inertia power networks," *IET Gener., Transmiss. Distribution*, vol. 13, no. 9, pp. 1520–1526, May 2019, doi: 10.1049/iet-gtd.2018.5542.
[25] GAMS Development Corporation. (Nov. 11, 2023). *GAMS Documentation*. [Online]. Available: https://www.gams.com/latest/docs/index.html
[26] F. Arredondo, P. Ledesma, and E. D. Castronuovo, "Optimization of the operation of a flywheel to support stability and reduce generation costs using a multi-contingency TSCOPF with nonlinear loads," *Int. J. Electr. Power Energy Syst.*, vol. 104, pp. 69–77, Jan. 2019, doi: 10.1016/j.ijepes.2018.06.042.
[27] IT Institute and University of Illinois Urbana-Champaign, *Illinois Center for a Smarter Electric Grid-Power Cases*. Accessed: Oct. 27, 2023. [Online]. Available: https://icseg.iti.illinois.edu/power-cases/
[28] P. Ledesma, F. Arredondo, and E. D. Castronuovo. *GAMS Transient Stability-Constrained Optimal Power Flow Model of the IEEE 39 Bus Test Case Including Non-Synchronous Generation—Repositorio de Datos UC3M*. Accessed: May 25, 2022. [Online]. Available: https://edatos.consorciomadrono.es/dataset.xhtml?persistentId=doi:10.21950/ZPRADY
[29] P. Ledesma, I. A. Calle, E. D. Castronuovo, and F. Arredondo, "Multi-contingency TSCOPF based on full-system simulation," *IET Gener., Transmiss. Distribution*, vol. 11, no. 1, pp. 64–72, Jan. 2017, doi: 10.1049/iet-gtd.2016.0355.
[30] F. Arredondo, E. Castronuovo, P. Ledesma, and Z. Leonowicz, "Analysis of numerical methods to include dynamic constraints in an optimal power flow model," *Energies*, vol. 12, no. 5, p. 885, Mar. 2019, doi: 10.3390/en12050885.
[31] W. W. Price et al., "'Load representation for dynamic performance analysis," *IEEE Trans. Power Syst. (Inst. Elect. Electron. Eng.);(United States)*, vol. 8, no. 2, 1993.

FRANCISCO ARREDONDO received the Ph.D. degree in electrical engineering from Universidad Carlos III de Madrid, in 2019. He is currently an Assistant Professor with Universidad Carlos III de Madrid. He has been an Academic Visitor with the Wroclaw University of Technology, Poland. His research interests include the power system stability, renewable generation, energy storage systems, and mathematical optimization methods.

MICHAIL RACHMANIDIS received the integrated master's degree in electrical engineering from the University of Patras, in 2022. In 2021, he was an Assistant Researcher with Universidad Carlos III de Madrid. Currently, he is a Researcher with DSS Laboratory, EPU-NTUA. His research interests include power systems analysis, renewable energy integration, and smart grid technologies.

PABLO LEDESMA received the Ph.D. degree from Universidad Carlos III de Madrid, in 2001. He is currently an Associate Professor with Universidad Carlos III de Madrid. He was with the Spanish TSO, on several projects on large-scale integration of renewable energy. He has been an Academic Visitor with Chalmers University, Sweden, and Strathclyde University, U.K. His areas of research are transient stability and dynamic modeling of power systems.

EDGARDO D. CASTRONUOVO (Senior Member, IEEE) received the B.S. degree in electrical engineering from the National University of La Plata, Argentina, in 1995, and the M.Sc. and Ph.D. degrees from the Federal University of Santa Catarina, Brazil, in 1997 and 2001, respectively, and the Postdoctoral degree from INESC-Porto, Portugal, in 2005. He performed research periods with the Polytechnic of Milan, Italy, and CentraleSupélec, France. He was with CEPEL, Brazil, and INESC-Porto, worked on power system areas. Currently, he is a Full Professor with the Department of Electrical Engineering, Universidad Carlos III de Madrid, Spain. His interests are in optimization methods applied to power system problems, renewable generation, and storage.

MOHAMMADAMIN AGHAHASSANI received the Ph.D. degree in electrical engineering from Universidad Carlos III de Madrid, Spain, in 2023. He was a Visiting Researcher with University College Dublin, Ireland, in 2022. He is currently a Postdoctoral Researcher with Universitat Politècnica de Catalunya (CITCEA-UPC), Spain. His research interests include power system modeling and simulation and grid integration studies.